Multi-Wavelength Fluorescence-Quenching Model for Determination of Cu^{2+} Conditional Stability Constants and Ligand Concentrations of Fulvic Acid

MICHAEL D. HAYS,* DAVID K. RYAN, and STEPHEN PENNELL

United States Environmental Protection Agency, National Risk Management Research Laboratory, Research Triangle Park, North Carolina 27711 (M.D.H.); University of Massachusetts Lowell, Department of Chemistry, Lowell, Massachusetts 01854 (D.K.R.); and University of Massachusetts Lowell, Department of Mathematics, Lowell, Massachusetts 01854 (S.P.)

In this work, a multi-wavelength model (MWM) is developed. It uses fluorescence bands in the fulvic acid (FA) spectrum that quench upon binding of inorganic Cu^{2+} to FA. Quenching data at pH values of 5, 6, and 7 are placed in sets, containing fluorescence measures at select wavelengths versus added copper (C_M). Intensity data of wavelength set 1 are obtained from 25 nm constant offset synchronous fluorescence spectra (SyF), in which are observed distinct peaks (λ_{ex} = 415 nm, λ_{em} = 440 nm; and λ_{ex} = 471 nm, λ_{em} = 496 nm). Wavelength set 2 intensity data are obtained from the FA fluorescence excitation and emission maxima (λ_{ex} = 335 nm, λ_{em} = 450 nm; and λ_{ex} = 471 nm, λ_{em} = 496 nm). Application of MWM shows that the multi-wavelength data sets characterize ligands of different binding strength (log K_x) and concentration (C_{Lx}). Corresponding to pH values of 5, 6, and 7, mean and standard deviation values for wavelength set 1 are log $K_{415/440}$ = 4.66 (0.12), 5.03 (0.12), and 5.05 (0.08), log $K_{471/496}$ = 4.93 (0.06), 5.27 (0.11), and 5.39 (0.09), $C_{415/440}$ = 3.1 (1.5), 10.9 (4.5), and 7.9 (3.9) μM, $C_{471/496}$ = 14.3 (3.0), 1.7 (0.6), and 1.4 (0.5) μM. And for wavelength set 2, log $K_{335/450}$ = 4.50 (0.03), 4.96 (0.27), and 5.22 (0.08), log $K_{471/496}$ = 5.02 (0.04), 5.42 (0.32), and 5.71 (0.09), $C_{335/450}$ = 8.8 (0.5), 21.9 (7.9), and 18.7 (0.3) μM, $C_{471/496}$ = 21.0 (2.5), 7.17 (1.2), and 7.09 (0.3) μM. The ability of the 415/440 nm SyF transect to characterize the main excitation and emission maximum of FA at 335/440 nm is evaluated. Relatively low concentration values returned by the model for this transect (415/440 nm) suggest that it is not entirely illustrative of the maximum. The model predictive capability is verified at pH 6 with two fluorescing Cu^{2+} chelating organic compounds, L-tyrosine and salicylic acid. This test confirms that the model is capable of providing good estimates of equilibrium binding parameters from multi-wavelength measurements of a mixed ligand system.

Index Headings: **Fulvic acids; Cu(II); Fluorescence quenching; Conditional stability constants; Multi-wavelength model.**

INTRODUCTION

Fulvic acids (FA) are complex mixtures of macromolecules found in soils and natural waters.[1] Classified as the fraction of organic matter soluble at both high and low pH, FA play an important role in the speciation of copper in aquatic systems.[2] Studies show that in its free form, copper (Cu^{2+}) can be toxic to aquatic biota.[3–6] This toxicity can be moderated or completely eliminated provided that the Cu^{2+} coordinates with FA.[5,7] Aside from regulating bioavailability, FA alter fate and transport of Cu^{2+} in groundwater because of their capacity to adsorb to mineral surfaces that partition Cu^{2+}.[8] Accordingly, accurate determination of complexation strength between dissolved FA and potentially toxic Cu^{2+} as well as organic ligand concentrations in FA is essential.

Fluorescence spectroscopy is a nondestructive analytical technique that effectively determines Cu^{2+}–FA conditional stability constants and ligand concentrations by virtue of the proportionality between signal intensity and the free ligand concentration.[9–15] However, use of FA fluorescence for quantitative study of complexation requires that proportionality is independently verified, as is the case for the FA sample used here (isolated by Weber). This verification is made necessary on account of Cook and Langford,[16] whose efforts with a Laurentian FA show that it is possible for bound copper to exceed total copper added while implementing a fluorescence approach. This work stands supported by several prior light-scattering and fluorescence studies,[17,18] which introduce the possibility of a cooperative effect due to bridged complex (CuL_2) and ''pseudochelation''. The latter is a delicate association with metal by ligand eventually yielding complex and expected to show a [Cu^{2+}] dependence more detailed than a simple linear relationship can describe. Still, fluorescence spectroscopy has several advantages over separation methods used to study Cu^{2+}–FA complexation because it is not plagued by loss of material due to adsorption or by disruption of the equilibrium, is capable of high sensitivity, and does not require the adjustment of ionic strength or addition of other reagents for analysis. Fluorescence is also unique among metal speciation methods in that it measures a property of the ligand that changes with complexation rather than measuring free and bound metal.

Synchronous scan fluorescence (SyF) spectroscopy in particular is powerful because of its ability to detect multiple fluorophores in a single spectrum.[19] Past work demonstrates that Cu^{2+} induces quenching of multiple FA fluorophores in SyF spectra.[20–22] These fluorophores exhibit varying degrees of quenching at independent wavelengths and are thought to be characteristic of different ligand sites. Additional work with FA assigns fluorescence lifetimes to resolved SyF peaks, showing at least two components that bind Cu^{2+} with different strengths.[16]

Although fluorescence data support the presence of multiple Cu^{2+} binding sites in FA, there are still few multi-site models developed to use fluorescence to evaluate solution equilibria.[23,24] And although useful qualitatively, SyF is subject to certain quantitative limitations. The SyF spectrum may sample only a section of a fluorescence peak or might even miss a fluorophore completely, depending on what constant offset ($\Delta\lambda$) value is used.[25]

Received 1 April 2002; accepted 22 November 2002.
* Author to whom correspondence should be sent.

0003-7028/03/5704-0454$2.00/0
© 2003 Society for Applied Spectroscopy

Therefore, because $\Delta\lambda$ is not likely to be optimum for all peaks in any given experiment, it remains uncertain if the SyF spectra of FA are sensitive enough to measure the total possible quenching response due to copper addition. For these reasons, a multi-wavelength model (MWM) is developed to use the fluorescence response at multiple wavelengths to quantify copper binding by FA.

THEORY

Multi-Wavelength Model Development. The MWM model framework corresponds to the multi-site treatment of Stern–Volmer,[26,27] which assumes that more than one component characterizes fluorescence and withdraws from the pool of added quencher. However, in contrast with the Stern–Volmer multi-site treatment, the MWM does not delineate overlapping fluorescence component fractions. It instead considers them resolved and presumes unity for the fraction of each component contributing to the unquenched fluorescence signal intensity.

As dissolved FA binds Cu^{2+}, quenching of the two fluorophores is exhibited by a static mechanism.[28] Assuming that these fluorophores characterize separate 1:1, Cu^{2+} : ligand binding sites, the equilibria can be expressed with charges omitted for simplicity:

$$M + L1 \leftrightarrows ML1$$

$$M + L2 \leftrightarrows ML2$$

L1 and L2 are the metal-free ligand sites (in all forms, both protonated and unprotonated) corresponding to fluorophores 1 and 2. ML1 and ML2 are the metal-bound species at these sites, and M is the free metal in solution. MWM can be extended to describe metal binding by more than two components by simply including additional terms. In this attempt to better define the Cu–FA system in a mathematical sense, it is possible that the binding sites of FA may not in every case function independently. Induced chelation (bridged complexing) or cooperativity between sites due to metal loading are possible and likely bring about conformational change. With the relationship between fluorescence change and conformational reorganization of FA not yet perfectly understood, exact modeling of this relationship is not yet accomplished but will advance with future work.

For fluorophores 1 and 2, 1:1 conditional stability constants (K_1 and K_2) are introduced:

$$K_1 = [ML1]/[M][L1] \quad (1)$$

$$K_2 = [ML2]/[M][L2] \quad (2)$$

Even if not perfectly ideal, K_1 and K_2 classify average bulk properties of the ligand site array.[9]

Mass balance equations for both metal and ligand are:

$$C_M = [M] + [ML1] + [ML2] \quad (3)$$

$$C_{L1} = [L1] + [ML1] \quad (4)$$

$$C_{L2} = [L2] + [ML2] \quad (5)$$

C_M is the known total added metal concentration, and C_{L1} and C_{L2} are total ligand site concentrations in solution, respectively. Equations 1 and 4 combine to give Eq. 6:

$$[ML1] = K_1C_{L1}[M]/(K_1[M] + 1) \quad (6)$$

Likewise, Eqs. 2 and 5 combine to give Eq. 7:

$$[ML2] = K_2C_{L2}[M]/(K_2[M] + 1) \quad (7)$$

The equations associating fluorescence and solution equilibria are as follows:

$$(I_{L1} - I_1)/(I_{L1} - I_{RES1}) = K_1[M]/(1 + K_1[M]) \quad (8)$$

$$(I_{L2} - I_2)/(I_{L2} - I_{RES2}) = K_2[M]/(1 + K_2[M]) \quad (9)$$

Equations 8 and 9 were derived with fundamental fluorescence quantum efficiency-concentration relationships developed in Ryan's original model.[29] I_1 and I_2 are the fluorescence intensity values measured at two separate excitation–emission wavelengths. We assume that before adding Cu^{2+}, $I_{L1} = I_1$ and $I_{L2} = I_2$. I_{L1} and I_{L2} are treated as constants to which all other measured intensity values are related. Once quenching terminates, the residual fluorescence intensity parameters (I_{RES1} and I_{RES2}) characterize the remaining fluorescence signal at the wavelengths of the set.

Substituting Eqs. 6 and 7 into Eq. 3 yields:

$$C_M = [M] + K_1C_{L1}[M]/(K_1[M] + 1) + K_2C_{L2}[M]/(K_2[M] + 1) \quad (10)$$

Multiplying through by $(K_1[M] + 1)(K_2[M] + 1)$ gives the following third-order polynomial:

$$K_1K_2[M]^3 + \{K_1K_2(C_{L1} + C_{L2} - C_M) + K_1 + K_2\}[M]^2 + \{C_{L1}K_1 + C_{L2}K_2 - C_M(K_1 + K_2) + 1\}[M] - C_M = 0 \quad (11)$$

Equations 8, 9, and 11 predict the fluorescence intensity values I_1 and I_2 corresponding to a given value of the added metal concentration (C_M). We first solve Eq. 11 numerically to find the value of free metal concentration [M], then we use Eqs. 8 and 9 to calculate I_1 and I_2. Of the eight parameters in this model, two (I_{L1} and I_{L2}) are measured experimentally and six (K_1, K_2, C_{L1}, C_{L2}, I_{RES1}, and I_{RES2}) are estimated numerically using the standard least-squares procedure. We measure the values of I_1 and I_2 corresponding to several different values of C_M, and we then choose the values of K_1, K_2, C_{L1}, C_{L2}, I_{RES1}, and I_{RES2} so as to minimize the sum of squares of the differences between the experimentally measured intensity values and the intensity values predicted by the model. Because of measurement error, there is no way to find the exact parameter values. The method of least squares is a standard procedure for finding a set of parameter values which best fit the experimental data.

EXPERIMENTAL

Apparatus. A Farrand Mark 1 spectrofluorometer (Farrand Optical Company Inc., Valhalla, NY) was used to obtain fluorescence data. The instrument was equipped with two grating monochromators with slits set for 5-nm excitation and 10-nm emission bandpass, a 150 watt xenon arc lamp, and a photomultiplier tube. Wavelength and intensity data from the analog output of the instrument were fed to an analog/digital board (Metrabyte, Kiethly, Taunton, MA) and processed using several pro-

grams written in BASIC. Data were viewed on a personal computer (Dell Dimension, Dell Computer Corporation, Austin, TX) running GRAMS/386 software (V2.0, Galactic Industries, Salem, NH).

Titrations were performed in a temperature-jacketed titration cell fitted with a cap (Princeton Applied Research, EG & G, Princeton, NJ). Inserted through the top of the cap was a glass combination pH electrode (Ross 8104, Orion, Boston, MA) attached to an autochemistry system (960, Orion). A constant temperature water bath (VWR Scientific, Boston, MA) maintained solution temperature at 25 °C (±2 °C). Transfer of solution from the titration cell to the 10-mm quartz cuvette (NSG Precision Cells, Farmingdale, NY) and reagent additions were made manually by pipette (Brinkmann Instruments Inc., Westbury, NY).

Reagents. The source of FA may very well govern the relationship between Cu^{2+} complexation and quenching. A well characterized[30,31] FA isolated from the B_2 horizon of a podzol soil was obtained from Dr. James Weber (Department of Chemistry University of New Hampshire, Durham, NH) and used here. Within the experimental C_M range, a linear relation between Cu^{2+} complexation and quenching was verified for this FA,[9] justifying its use in developing the MWM. This linear correlation was also apparent for humic-metal systems of natural waters.[10] For use in this study, all FA solutions were prepared in distilled deionized water (17 MΩ, Barnstead-Nanopure) to prevent interference from other FA-binding cations and filtered through 0.4 μm polycarbonate filters (Costar Corp., Cambridge, MA).

The L-tyrosine (Tyr) (Aldrich Chemical Co., Milwaukee, WI) and salicylic acid (Sal) (Fisher Scientific Co, Pittsburgh, PA) stock solutions were prepared in deionized water made basic with NaOH (1 M), stirred (~2 h), and neutralized with perchloric acid (1 M). A fresh mixture of Sal (70 μM) and Tyr (35 μM), prepared from individual stock solution aliquots, was used for each model compound titration. Appropriate amounts of reagents were added to FA and to model compound solutions to maintain ionic strength (0.1 M, $NaClO_4$) and pH (from 5 to 7, NaOH and $HClO_4$) constant.

The Cu^{2+} standard was prepared from reagent grade perchlorate salt and standardized by direct current plasma atomic emission spectrometry (Applied Research Laboratory, Valencia, CA) versus commercial standards.

Fluorescence Titration Procedure. A comprehensive description of the procedure used here was described elsewhere.[9] Briefly, in a titration cell, the pH of a continuously stirred solution (50 mL) of dissolved FA (15 mg/L) was adjusted to within 0.02 pH units of the desired value. Following an equilibration period (8–10 min), the solution (1 mL) was transferred from the titration cell to the quartz cuvette and transferred back to the cell as a rinse. An aliquot (2 mL) of solution was then delivered to the cuvette, fluorescence measurements at appropriate wavelengths were taken, and the solution was transferred back to the titration cell. A second set of fluorescence measurements at the same wavelengths was taken after a micromolar aliquot of Cu^{2+} was delivered to the titration cell, the pH readjusted, and the solution equilibrated. These steps were repeated until complete titration curves for each wavelength set were generated.

Soil Fulvic Acid Fluorescence Measurements. Excitation and emission spectra as well as $\Delta\lambda = 25$ nm SyF were collected for FA solutions at pH values of 5, 6, and 7. SyF wavelength maxima, $\lambda_{ex} = 415$ nm, $\lambda_{em} = 440$ nm (415/440 nm); and $\lambda_{ex} = 471$ nm, $\lambda_{em} = 496$ nm (471/496 nm), were utilized. The excitation and emission maxima were observed at $\lambda_{ex} = 335$ nm, $\lambda_{em} = 450$ nm (335/450 nm); and $\lambda_{ex} = 471$ nm, $\lambda_{em} = 496$ nm (471/496 nm). Measurements were placed into sets (1) wavelength set 1, 415/440 nm and 471/496 nm and (2) wavelength set 2, 335/450 nm and 471/496 nm. Each set was modeled separately with MWM. We assessed the ability of 415/440 nm SyF maximum, a cross-section of the 335/440 nm excitation and emission maximum, to measure quenching and, in turn, binding at the main fluorescence component (335/440 nm).

Model Compound Fluorescence Measurements. The fluorescence excitation and emission maxima of Sal and Tyr were observed at $\lambda_{ex} = 317$ nm, $\lambda_{em} = 404$ nm; and $\lambda_{ex} = 277$ nm, $\lambda_{em} = 296$ nm, respectively. Modeling input data were acquired at pH 6 using $\Delta\lambda = 50$ nm SyF. This offset was determined to be optimum for monitoring the Sal and Tyr fluorescence.

Data Treatment. The details of implementation of the MWM curve-fitting operation will be described extensively.[32] Briefly, the curve-fitting routine was implemented using a Nelder–Meade simplex algorithm in Matlab (Math Works Inc., Natick, MA).[33] A computer program was designed, in which the parameter values K_1, K_2, C_{L1}, C_{L2}, I_{RES1}, and I_{RES2} were chosen so as to minimize the sum of the squares of the differences between experimental intensity values and values predicted by the model. A numerical solution for M was calculated using Eq. 11 and the ROOTS command in Matlab. Only one positive real root exists for Eq. 11.

RESULTS AND DISCUSSION

Fluorescence Titrations of Model Compounds. To assess the predictive capability of the MWM, Sal and Tyr are titrated with Cu^{2+}. Although not perfectly representative of the entire complex FA ligand mixture, these compounds exhibit fluorescence behavior and carboxyl and phenolic functionalities similar to the FA sample used here.[28] Also, as evidenced by electron spin resonance analysis, the FA used here primarily comprises aromatic moieties in the form of semiquinone-like structures,[34] attesting to the refractory nature of FA. Though useful for this work, extension of the chemical properties of these model compounds to typify all FA samples may not be reasonable. Arrays of macromolecular structures in the FA sample likely depend on its source. It should also be clear that these model compounds cannot mimic all binding stoichiometries (such as growth of a metal chelate from independent sites), aggregate forms, and conformational properties of FA, particularly at high metal loadings.

For replicate Cu^{2+} titrations ($N = 3$) of fluorescent Sal and Tyr, Table I lists the mean conditional stability constant (log K_1 and K_2) and ligand concentration values (C_{L1} and C_{L2}) and their experimental standard deviations as predicted by the MWM. These MWM estimates reveal that Cu^{2+} complexes Tyr more strongly than Sal. And

TABLE I. MWM calculated equilibrium parameters for a mixture of the two model compounds.[a]

Model compound	Conditional log K from literature ref. 24	MWM calculated log K	Experimental C_L (μM)	MWM calculated C_L (μM)	MWM calculated I_{RES} (μM)
Sal	3.20	3.76 (±0.14)	70.0 μM	65.8 (±47.2)	15.9 (±8.6)
Tyr	4.55	4.79 (±0.16)	35.0 μM	14.9 (±6.6)	2.4 (±0.5)

[a] Standard deviations are in parentheses.

consistent with the model framework, a larger percentage of Tyr fluorescence is quenched (data not shown). Closer analysis shows that mean log K values of Tyr and Sal are within 5 and 20% of their respective theoretical conditional stability constant values, which are calculated using the experimental pH of 6, each species' pK_a, and thermodynamic stability constants.[35] The high average MWM-approximated log K value for the Cu–Sal complex may be due to the moderate fluorescence change caused by the weak complexation of Cu^{2+} by Sal. As expected, the calculated average value of C_L for Sal is within 6% of its experimentally fixed concentration, whereas the average calculated C_L value for Tyr is estimated as approximately half of its experimental value. For the latter result, formation of a 2:1 Tyr–copper complex seems evident.[36]

The relatively high I_{RES} value for Sal indicates that it is in its free form near the titration end. In marked contrast, the low I_{RES} value for Tyr suggests that quenching is nearly complete and essentially all the Tyr is bound at high C_M. Examination of the curve-fitting results shows that values of log K calculated for Sal and Tyr are well within the acceptable uncertainty range of ±0.25 log units. MWM predictions generally agree well with theory and verify that the multi-wavelength measurements of a mixed ligand system may be used to estimate coordination strength and ligand capacity for Cu^{2+}.

Fluorescence Quenching of Wavelength Set 1. The $\Delta\lambda$ = 25 nm SyF of our soil FA contains a 415/440 nm peak, which transects the excitation and emission maximum (335/440 nm), and the 471/496 nm maximum, which make up wavelength set 1. Figure 1 shows the effect at pH 6 of 0–60 μM Cu^{2+} on the FA SyF spectra (15 mg/L). The narrow 471/496 nm component is more rapidly quenched than the broader, less intense 415/440 nm peak, an indication that these two fluorophores represent ligands that uniquely complex Cu^{2+}. This pattern is observed at all pHs studied. Figure 2 provides the fluorescence titration data at pH 5 at these wavelengths. These data (Fig. 2) (1) verify the difference in the degree of quenching at each wavelength, (2) show that a large proportion of the quenching occurs at high ligand-to-Cu^{2+} ratios (low Cu^{2+} loadings) as expected, and (3) show titration data in agreement with the MWM-predicted values (solid lines).

Table II gives MWM-predicted mean and standard deviation values of log K_1, log K_2, C_{L1}, C_{L2}, I_{RES1}, and I_{RES2} from replicate titrations (N = 3) at pH values of 5, 6, and 7. At each pH, log K_2 (471/496) > log K_1 (415/440), confirming that the 471/496 nm fluorophore characterizes stronger binding organic ligands. Estimates show that log K_1 (415/440) and log K_2 (471/496) increase as a function of pH; however, the increase is negligible from pH 6 to 7. Perhaps ligand sites in our FA are completely deprotonated across this range, thereby lessening the influence of pH on the log K_1 and K_2 values. Alternatively, this result may be due to the omission of formed Cu–hydroxy species from model calculations at pH 7, which in effect decreases the [Cu^{2+}] available to coordinate to ligand sites.

Because C_{L1} = [L1] + [ML1], model-obtained values

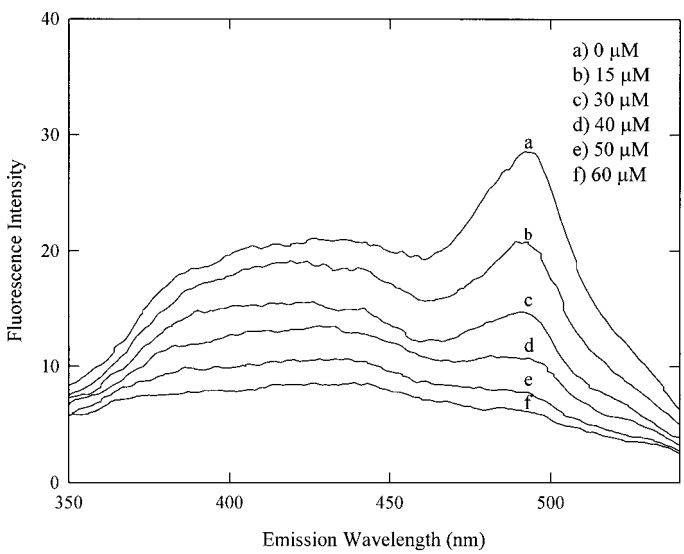

FIG. 1. A set of 25 nm constant offset synchronous fluorescence spectra of 15 mg/L soil FA at 0.1 M ionic strength, 25 °C, and pH 6 as a function of total added copper, C_M.

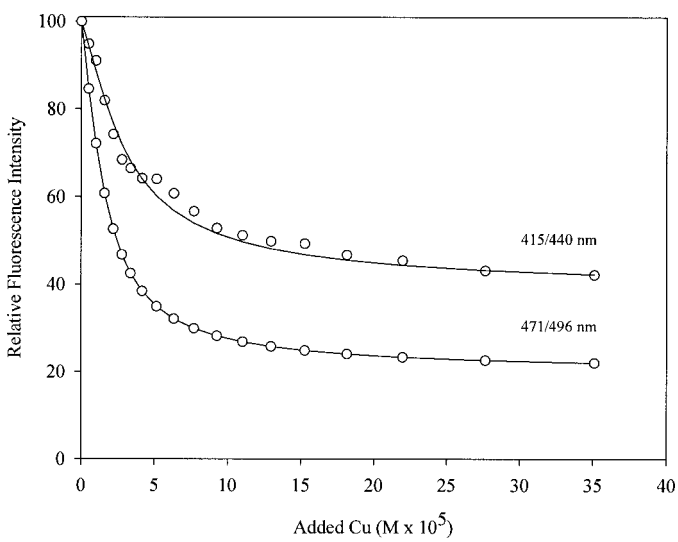

FIG. 2. Wavelength set 1 fluorescence quenching data (○) and model-fitted curves (as solid lines) for the Cu^{2+} titration of 15 mg/L FA at 0.1 M ionic strength, 25 °C, and pH 5.

TABLE II. MWM calculated equilibrium parameters for wavelength set 1 of FA.[a]

pH	log K_1 415/440	log K_2 471/496	C_{L1} 415/440 (μM)	C_{L2} 471/496 (μM)	I_{RES1} 415/440	I_{RES2} 471/496
5	4.66 (±0.12)	4.93 (±0.06)	3.1 (±1.5)	14.3 (±3.0)	39.2 (±1.7)	20.2 (±1.2)
6	5.03 (±0.12)	5.27 (±0.11)	10.9 (±4.5)	1.7 (±0.6)	27.6 (±2.5)	15.7 (±0.5)
7	5.05 (±0.08)	5.39 (±0.09)	7.9 (±3.9)	1.4 (±0.5)	27.6 (±7.0)	16.9 (±5.0)

[a] Standard deviations are in parentheses.

of C_{L1} should be equal despite pH. The same is also valid for C_{L2} (471/496), C_{L2} = [L2] + [ML2]. MWM-determined mean values of C_{L1} and C_{L2} at pH values of 6 and 7 correspond to within 28 and 18%. Because C_{L1} (415/440) > C_{L2} (471/496) at these pH values, a lower concentration of stronger binding ligands is assigned to the 471/496 nm fluorophore. At pH 5, $C_{L2} > C_{L1}$, and I_{RES1} increases by a factor of two when compared with I_{RES1} values at pH values of 6 and 7. Ryan and Weber[9] had difficulty modeling fluorescence titration data at pH 5 with the same FA used here. A single data set that was treated at this pH provided a relatively high I_{RES} of 40.2. This value is nearly identical to the I_{RES1} of 39.2 ± 1.7 calculated here and suggests that significant levels of molecules are in solution that (1) fluoresce but do not complex, (2) fluoresce, complex, and quench only partially, or (3) fluoresce, complex, and do not undergo quenching. Only type (3) material remains unaccounted for by the model. Curve-fitting results show that I_{RES1} (415/440) > I_{RES2} (471/496) at each pH; fluorophore 2 exhibits a higher degree of quenching. At all pH values, the calculated averages of I_{RES2} (471/496) are similar, indicating that termination of quenching at this peak is independent of pH.

Fluorescence Quenching of Wavelength Set 2. The fluorescence excitation–emission maxima (335/450 nm and 471/496 nm) combine to form wavelength set 2. At these selected wavelengths, fluorescence titration data at pH 5 are given (Fig. 3). The measured quenching provides added support for the presence of individual components with distinct fluorescence and coordination characteristics. Compared with the 335/450 nm maximum, quenching at 471/496 nm advances more rapidly at lower C_M loadings (C_M < 10 μm). As the titration proceeds (C_M > 10 μm), the quenching observed at 335/450 nm exceeds that at 471/496 nm. Near the titration end (C_M > 25 μm), the relative fluorescence at these wavelengths is essentially equal.

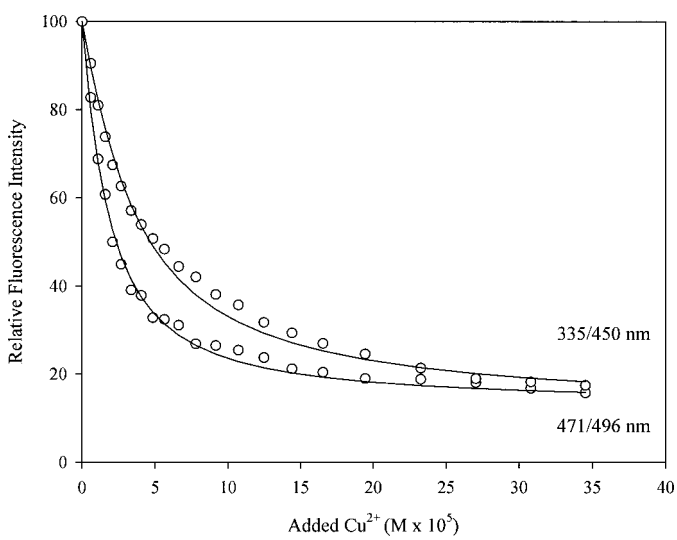

FIG. 3. Wavelength set 2 fluorescence quenching data (○) and model-fitted curves (as solid lines) for the Cu^{2+} titration of 15 mg/L FA at 0.1 M ionic strength, 25 °C, and pH 5.

The MWM-predicted logarithmic values of K_1 (335/450) and K_2 (471/496) at wavelength set 2 increase with pH on average (Table III). In addition, log K_1 (335/450) < log K_2 (471/496) at each pH, verifying that the molecules excited at longer wavelengths bind Cu^{2+} more strongly. Mean C_{L1} (335/440) values at pH values of 6 and 7 agree to within 15%, and across the same pH range C_{L2} (471/496) values agree to within 10% of one another, where C_{L1} (335/440) > C_{L2} (471/496). Modeling at the maxima did not correct the reverse trend ($C_{L2} > C_{L1}$) at pH 5, which is also observed at wavelength set 1. I_{RES1} at pH 5 is 2-fold greater than both of the pH 6 and 7 values, which are virtually identical. Data of both wavelength sets show that this increase in the model-estimated value of I_{RES1} causes a significant decrease in C_{L1}, marking a potential artifact in modeling C_{L1}.

Figure 3 shows the MWM predictions (solid lines). For the 335/450 nm peak, they deviate from the experimental data, particularly midway through the titration. This variation is also observed at pH values 5–7 and for the 415/440 nm peak. Perhaps the oversimplification inherent in the 1:1 coordination ratio assumption or overlap of fluorescent components at the 335/450 nm maximum explain this difference. Cook and Langford[16] support the latter interpretation. Their work establishes that multiple fluorophores that respond differently to Cu^{2+} are the basis of a nonlinear relationship between complex formation and fluorescence response at the excitation and emission maximum. This implies that two or more overlapping fluorophores make up the excitation and emission maximum (335/440 nm) of FA even though only a single broad band is evident. It is unclear if the 471/496 nm maximum is actually the second overlapping component. Regardless, the MWM would not properly treat this case because it recognizes just one fluorescence component per peak. Moreover, linearity between complexation and quenching is assumed here, but shielding of binding sites or fluorescence, conformational effects, or the possibility of metal : ligand ratios other than the 1:1 ratio handled by the model may cause subtle nonlinearity between the quenching and complexation.[17,18] It also is expected that these effects are highly dependent on the origin of FA. Therefore, in the event that independent evidence supports any of these cases, caution in applying and interpreting results of this model (MWM) is justified.

Comparison of Wavelength Sets 1 and 2. The mon-

TABLE III. MWM calculated equilibrium parameters for wavelength set 2 of FA.[a]

pH	log K_1 335/440	log K_2 471/496	C_{L1} 335/440 (μM)	C_{L2} 471/496 (μM)	I_{RES1} 335/440	I_{RES2} 471/496
5	4.50 (±0.03)	5.02 (±0.04)	8.8 (±0.5)	17.6 (±2.5)	21.0 (±1.5)	21.4 (±4.1)
6	4.96 (±0.27)	5.42 (±0.32)	21.9 (±7.9)	1.3 (±1.2)	7.17 (±5.6)	15.5 (±3.4)
7	5.22 (±0.08)	5.71 (±0.09)	18.7 (±0.3)	1.2 (±0.3)	7.09 (±3.7)	19.8 (±3.7)

[a] Standard deviations are in parentheses.

itoring position of fluorophore 1 (415/440 nm and 335/450 nm) is the principle difference between the wavelength sets. It is postulated that the 415/440 nm measurement transects and is thus characteristic of the excitation and emission maximum (335/450 nm). Assessing model results for fluorophore 1 of wavelength sets 1 and 2 should serve to evaluate the potential of the 415/440 nm peak in the SyF to represent the maximum. For the different wavelength sets, curve-fitting results show at each pH that log K_1 (415/440 nm and 335/440 nm) values (Tables II and III) are within 5%. Fluorophore 2 shows the identical result for log K_2, because both wavelength sets use the 471/496 nm fluorescence maximum. For this same reason, MWM predictions of C_{L2} (471/496) are within 25% across wavelength sets 1 and 2. However, by at least two-fold, C_{L1} (335/450) > C_{L1} (415/440) at the pH values examined. Apparently, additional ligand molecules are excited at the higher energy associated with fluorophore 1 as measured by wavelength set 2 (335/450 nm). This result combined with the high I_{RES1} values reported for 415/440 nm indicates that the FA SyF spectra ($\Delta\lambda$ = 25 nm) may not be entirely representative of component 1 quenching by Cu^{2+} (or of the excitation–emission maximum), potentially limiting the use of the $\Delta\lambda$ = 25 nm SyF to determine total ligand concentrations of this component at different pH values. In summary, measurements at 335/450 nm render an expanded characterization of the fluorescent ligand molecules present.

Literature Equilibrium Values. Literature-selected[13,20,21] conditional stability constant and ligand concentration values for Cu^{2+}–FA at varying pH values are listed in Table IV. The quenching data used to generate these estimates[13,20,21] are obtained with different scanning methods,[13] wavelengths, component analysis routines, and FA samples.[20,21] Because the FA concentrations used during titration experiments carried out by these investigators[13,20,21] are in some cases orders of magnitude greater than those used in our work, the ligand concentration estimates are normalized to 15 mg/L for ease of comparison.

TABLE IV. Literature conditional stability constant and ligand concentration values calculated from multi-wavelength fluorescence quenching data of Cu^{2+}-titrated soil FA.

Sample	Ref (#)	pH	log K_1	log K_2	C_{L1} (μM)	C_{L2} (μM)	I_{RES1}	I_{RES2}
Forest[a]	18[c]	5	3.95	4.51	3.1	3.3	5	1
Forest[a]	18[c]	6	4.03	4.57	7.1	13.0	0	0
Forest[a]	17[d]	6	4.92	5.57	15.0	4.5	na[f]	na[f]
Podzol[b]	13[e]	7	5.22	5.64	7.3	4.8	11.4	4.3

[a] Isolated from a Portuguese forest soil in Louros, Famalicáo.
[b] Isolated from the B_2 horizon of a Podzol soil (same material used in this study).
[c] Equilibrium estimates determined using $\Delta\lambda$ = 20 nm SyF together with self-modeling mixture analysis.
[d] Equilibrium estimates determined using $\Delta\lambda$ = 20 nm SyF together with evolving factor analysis.
[e] Equilibrium estimates determined using short and long wavelength maxima.
[f] Data not available.

With the exception of the pH 7 case,[13] in which the FA sample is the same as that used in this work, a FA isolated from a Portuguese forest soil is used, and quenching of $\Delta\lambda$ = 20 nm SyF spectra are deconvoluted to obtain signature bands used in modeling groups of Cu^{2+} binding molecules. In comparing the outcomes at pH 7, it can be seen that the conditional stability constants obtained for wavelength set 2 (Table III) agree well with the work of Seritti et al.[13] because the same FA material and wavelengths for collecting quenching data are used in both studies. The ligand concentration values calculated, however, show a significant difference and indicate that the modeling approaches used in these studies, although similar in principle, are not perfectly alike.

The equilibria values determined by Machado, et al.[21] significantly vary from those we report (Table II), as the origin of the FA, scanning offset, and modeling and analysis routines used are all different. Esteves da Silva and co-workers[20] calculate an added set of equilibria values using the same FA, scanning offset, and modeling protocol employed by Machado et al.[21] but implement an evolving factor analysis operation instead. These calculated values are in agreement (Table II) with those obtained here.

CONCLUSION

Evidence of two main fluorescence components in a well-characterized FA isolated from the B_2 horizon of a podzol soil is offered. Among other variables, the wavelength scanning procedure will effect how a fluorophore appears in a spectrum, which organic ligands are excited, and final titrimetric model estimates of solution equilibria. MWM-determined conditional stability constant and ligand concentration values provide features of copper-complexation by natural FA molecules at varying pH values for different multi-wavelength sets. Because quenching at the short wavelength (415/440 nm) peak in the SyF spectra of our FA terminates prior to the titration finish, accurate evaluation of the ligand concentration using this wavelength set proves challenging. This finding may impact investigations for which different wavelength scanning procedures are implemented to model metal complexation and solution equilibria. In summation, fluorescence quenching data in titrimetric form can be collected at representative multi-wavelength sets and used as input to the MWM model for calculation of conditional stability constant and ligand concentration values of FA. In each case, it is expected that the proportionality between

free ligand concentration and signal is independently verified.

ACKNOWLEDGMENTS

This work was carried out as part of the Ph.D. study of Michael D. Hays. The authors acknowledge the helpful discussions on fluorescence measurements with Dr. Chih-Ping Shia and Dr. Kuang-Pang Li. The authors also recognize and appreciate the helpfulness of the particular comments of an anonymous referee.

1. F. M. M. Morel and J. G. Hering, *Principles and Applications of Aquatic Chemistry* (John Wiley and Sons, New York, 1993), pp. 375–391.
2. M. Adhikari, G. Chakravorty, and G. C. Hazra, J. Indian Soc. Soil Sci. **20,** 311 (1972).
3. R. Petersen, Environ. Sci. Technol. **16,** 443 (1982).
4. J. P. Knezovich, F. L. Harrison, and J. S. Tucker, Arch. Environ. Contam. Toxicol. **10,** 241 (1981).
5. M. Y. Nor, *Humic Substances in the Global Environment and Implications on Human Health* (Elsevier Science B. V., New York, 1994), pp. 1055–1062.
6. W. J. Langston and G. W. Bryan, Proc. Int. Symp., 375 (1983).
7. D. M. Diks and H. E. Allen, Bull. Environ. Contam. Toxicol. **30,** 43 (1983).
8. A. P. Robertson and J. O. Leckie, Proc. Int. Symp., 487 (1994).
9. D. K. Ryan and J. H. Weber, Anal. Chem. **54,** 986 (1982).
10. D. K. Ryan and J. H. Weber, Environ. Sci. Technol. **16,** 866 (1982).
11. F. H. Frimmel and W. Hopp, Fresenius' J. Anal. Chem. **325,** 68 (1986).
12. L. S. Ventry, D. K. Ryan, and T. R. Gilbert, Microchem. J. **44,** 201 (1991).
13. A. Seritti, E. Morelli, L. Nannicini, A. Giambelluca, and G. Scarno, Sci. Tot. Environ. **148,** 73 (1994).
14. M. D. Hays, D. K. Ryan, and S. Pennell, *Humic/Fulvic Acids and Organic Colloidal Materials in the Environment* (American Chemical Society, Washington, D.C., 1996), pp. 108–124.
15. D. K. Ryan, C. P. Thompson, and J. H. Weber, Can. J. Chem. **61,** 1505 (1983).
16. R. L. Cook and C. H. Langford, Anal. Chem. **67,** 174 (1995).
17. A. W. Underdown, C. H. Langford, and D. S. Gamble, Environ. Sci. Technol. **19,** 132 (1985), and references therein.
18. A. W. Underdown, C. H. Langford, and D. S. Gamble, Anal. Chem. **53,** 2139 (1981), and references therein.
19. S. E. Cabaniss, Environ. Sci. Technol. **26,** 1133 (1992).
20. J. C. G. Esteves da Silva and A. A. S. C. Machado, Chemom. Intell. Lab. Syst. **27,** 115 (1995).
21. A. A. S. C. Machado, J. C. G. Esteves da Silva, and J. A. C. Maia, Anal. Chim. Acta **292,** 121 (1994).
22. A. A. S. C. Machado and J. C. G. Esteves da Silva, Chemom. Intell. Lab. Syst. **19,** 155 (1993).
23. S. S. Smith and J. R. Kramer, Anal. Chim. Acta **363,** 21 (1998).
24. J. Luster, T. Lloyd, G. Sposito, and I. V. Fry, Environ. Sci. Technol. **30,** 1565 (1996).
25. H. W. Latz, A. H. Ullman, and J. D. Winefordner, Anal. Chem. **50,** 2148 (1978).
26. M. R. Eftink and C. A. Ghiron, Anal. Biochem. **114,** 199 (1981).
27. C. N. Ho, G. Patonay, and I. M. Warner, Trends Anal. Chem. **5,** 37 (1986).
28. R. A. Saar, and J. H. Weber, Anal. Chem. **52,** 2095 (1980).
29. D. K. Ryan, Ph.D. Thesis, University of New Hampshire, Durham, New Hampshire (1982).
30. J. H. Weber and S. A. Wilson, Water Res. **9,** 1079 (1975).
31. S. A. Wilson and J. H. Weber, Chem. Geol. **19,** 285 (1977).
32. M. D. Hays, D. K. Ryan, and S. Pennell, Anal. Chim. Acta, paper to be submitted (2003).
33. J. A. Nelder and R. Mead, Comput. J. **7,** 308 (1978).
34. S. A. Wilson and J. H. Weber, Anal. Lett. **10,** 75 (1977).
35. A. E. Martell and R. M. Smith, *Critical Stability Constants* (Plenum Press, New York, 1982).
36. L. S. Ventry, *Metal Binding by Humic Materials: An Integrated High-Performance Liquid Chromatography and Fluorescence Quenching Study,* Ph.D. Thesis, Northeastern University, Boston, Massachusetts (1989).